Syntillas Release Ca^{2+} at a Site Different from the Microdomain Where Exocytosis Occurs in Mouse Chromaffin Cells

Ronghua ZhuGe,*† Valerie DeCrescenzo,* Vincenzo Sorrentino,‡ F. Anthony Lai,§ Richard A. Tuft,*† Lawrence M. Lifshitz,*† Jose R. Lemos,* Corey Smith,¶ Kevin E. Fogarty,*† and John V. Walsh Jr.*

*Department of Physiology, and †Biomedical Imaging Group, University of Massachusetts Medical School, Worcester, Massachusetts 01655; ‡Dipartimento di Neuroscienze, Università di Siena, 53100 Siena, Italy; §Wales Heart Research Institute, University of Wales College of Medicine, Cardiff CF14 4XN, United Kingdom; and ¶Department of Physiology and Biophysics, Case Western Reserve University, Cleveland, Ohio 44106-4970

ABSTRACT Spontaneous, short-lived, focal cytosolic Ca^{2+} transients were found for the first time and characterized in freshly dissociated chromaffin cells from mouse. Produced by release of Ca^{2+} from intracellular stores and mediated by type 2 and perhaps type 3 ryanodine receptors (RyRs), these transients are quantitatively similar in magnitude and duration to Ca^{2+} syntillas in terminals of hypothalamic neurons, suggesting that Ca^{2+} syntillas are found in a variety of excitable, exocytotic cells. However, unlike hypothalamic nerve terminals, chromaffin cells do not display syntilla activation by depolarization of the plasma membrane, nor do they have type 1 RyRs. It is widely thought that focal Ca^{2+} transients cause ''spontaneous'' exocytosis, although there is no direct evidence for this view. Hence, we monitored catecholamine release amperometrically while simultaneously imaging Ca^{2+} syntillas, the first such simultaneous measurements. Syntillas failed to produce exocytotic events; and, conversely, spontaneous exocytotic events were not preceded by syntillas. Therefore, we suggest that a spontaneous syntilla, at least in chromaffin cells, releases Ca^{2+} into a cytosolic microdomain distinct from the microdomains containing docked, primed vesicles. Ryanodine (100 μM) reduced the frequency of Ca^{2+} syntillas by an order of magnitude but did not alter the frequency of spontaneous amperometric events, suggesting that syntillas are not involved in steps preparatory to spontaneous exocytosis. Surprisingly, ryanodine also increased the total charge of individual amperometric events by 27%, indicating that intracellular Ca^{2+} stores can regulate quantal size.

INTRODUCTION

The existence of intracellular Ca^{2+} stores in neurons and other excitable cells is well established although their precise role remains controversial (1–4). In contrast to postsynaptic Ca^{2+} stores, those in nerve terminals have received scrutiny only in the last few years (2). Ca^{2+} stores in nerve terminals have now been implicated in long-term potentiation (5) and depression (6) and those in terminals or axons in the pathophysiology of spinal cord injury (7). Nevertheless their precise functions and the mechanisms by which they act are far from understood.

Interest in Ca^{2+} stores in terminals was given considerable impetus by the discovery, in cerebellar interneurons (8) and then in cultured hippocampal pyramidal neurons (9), of spontaneous, short-lived, focal Ca^{2+} transients due to release from Ca^{2+} stores via RyRs. At least some of these transients are thought to cause ''spontaneous'' transmitter release and therefore miniature postsynaptic potentials, especially those of unusually large magnitude (''maximinis''). However, because of technical difficulties with these preparations, there is no direct evidence to show whether such transients cause exocytosis (2).

Another approach to the study of Ca^{2+} stores in terminals is to employ isolated exocytotic structures, such as terminals from hypothalamic magnocellular neurons, which permit study of Ca^{2+} stores without the complications of postsynaptic structures or multicellular preparations. In these terminals we found highly localized, brief, spontaneous Ca^{2+} transients, which could be quantified using a ''signal mass'' approach and hence were found to resemble Ca^{2+} sparks in muscle cells in time course and magnitude (1). We designated these transients as Ca^{2+} syntillas (*scintilla*, L. spark, from a nerve terminal, a synaptic structure). The power of this approach was illustrated by the discovery that Ca^{2+} syntillas are increased in frequency (but not in magnitude) by depolarization in the absence of Ca^{2+} influx, the first demonstration of this mechanism in neurons.

We wondered whether other excitable exocytotic cells might also exhibit Ca^{2+} syntillas. Here we report for the first time syntillas in chromaffin cells, a widely used model system for the quantitative study of exocytosis (10). Chromaffin cells are useful because exocytosis can be monitored amperometrically, permitting the simultaneous recording of individual Ca^{2+} syntillas and single exocytotic events. This, as Collin et al. (2) point out in their insightful, recent review, is a critical next step in investigating the role of syntillas and similar transients, and here we carried out such simultaneous recordings. Quite unexpectedly, single Ca^{2+} syntillas do not trigger ''spontaneous'' exocytosis, suggesting the existence of several distinct Ca^{2+} microdomains in chromaffin cells. Moreover,

Submitted July 29, 2005, and accepted for publication December 8, 2005.

Address reprint requests to John V. Walsh, Dept. of Physiology, University of Massachusetts Medical School, Worcester, MA 01655. Tel.: 508-856-3360; Fax: 508-856-1840; E-mail: john.walsh@umassmed.edu.

0006-3495/06/03/2027/11 $2.00

doi: 10.1529/biophysj.105.071654

chromaffin cells have type 2 and perhaps type 3 RyRs but not type 1, the type linked to sensors of membrane potential in skeletal muscle. Correspondingly, Ca^{2+} syntilla frequency is not altered by membrane potential. Surprisingly, blocking RyRs increases the magnitude of spontaneous exocytotic events, i.e., quantal size.

MATERIALS AND METHODS

Cell preparation and experimental conditions

Tight-seal, whole cell recordings on chromaffin cells, freshly dissociated from adult Swiss Webster mice, were performed with an Axopatch-1D amplifier on the same day as isolation. Swiss Webster mice of either sex (6–8 weeks) were killed by an overdose of ketamine (50 mg/kg I.P.) in accordance with the IACUC guidelines at the University of Massachusetts Medical School. The adrenals were harvested, connective tissue and cortex removed, and the medullae were incubated in medium containing 30 unit/ml papain, 1 mM DTT, and 0.5 mg/ml BSA at 35°C for 30 min. The tissues were next transferred to a medium containing 3 unit/ml collagenase F and 0.5 mg/mL BSA, and incubated at 35°C for another 15 min. Finally, the tissues were agitated with a fire polished wide-bore glass pipette to release the chromaffin cells in a medium containing (in mM) 135 NaCl, 6 KCl, 1 $MgCl_2$, 0.1 $CaCl_2$, 0.2 EDTA, 10 mM HEPES, and 10 glucose (pH 7.3).

The patch pipette solution (mM) was: 0.05 K_5fluo-3 (Molecular Probes, Eugene, OR), 135 KCl, 2 $MgCl_2$, 30 Hepes, 4 MgATP, 0.3 Na-GTP, pH 7.2. Bath solution: 135 NaCl, 5 KCl, 10 Hepes, 10 glucose, 1 $MgCl_2$, and 2.2 $CaCl_2$, pH 7.2. Ca^{2+}-free bath solution: 135 NaCl, 5 KCl, 10 Hepes, 10 glucose, 0.2 EGTA, 1 $MgCl_2$, pH 7.2. For Ca^{2+}-free experiments, the cells remained in the Ca^{2+}-containing solution until the beginning of each experiment; the duration of Ca^{2+}-free protocol was ~15 min to prevent depletion of Ca^{2+} from internal stores (11).

Image acquisition and analysis

General

Fluorescence images using fluo-3 as a calcium indicator were obtained using a custom-built wide-field digital imaging system (11). Rapid imaging at 333 Hz (exposure, 3 ms) or 50 Hz (exposure, 10 ms) was made possible by equipping the system with a cooled high-sensitivity, charge-coupled device camera developed in conjunction with the Massachusetts Institute of Technology Lincoln Laboratory (Lexington, MA). The camera was interfaced to a custom-made inverted microscope, and the cells were imaged using a 100× Nikon 1.4 NA oil objective, giving a pixel size of 133 nm at the specimen. The 488-nm line of an Argon Ion laser (Coherent, Santa Clara, CA) provided wide-field fluorescence excitation, with a shutter to control exposure duration, and emission of the Ca^{2+} indicator was monitored at wavelengths >500 nm. Subsequent image processing and analysis was performed offline using a custom-designed software package, running on either a Silicon Graphics (Mountain View, CA) or Linux/PC workstation.

Signal mass

To assess the properties of individual Ca^{2+} syntillas and do so quantitatively, the signal mass approach was used, as conceptualized by Sun et al. (12) and developed for wide-field microscopy of Ca^{2+} sparks by ZhuGe et al. (13). The purpose of this approach is to obtain a measure of the total amount of Ca^{2+} released in a focal Ca^{2+} transient, as opposed to a measure of the Ca^{2+} concentration, by monitoring the total increase in fluorescence. A brief summary of the signal mass method, which is described in detail in ZhuGe et al. (13), is as follows. During a syntilla, free Ca^{2+} (diffusion coefficient, $D = 250\ \mu m^2/s$) and Ca^{2+} bound to fluo-3 ($D = 22\ \mu m^2/s$) (14) quickly diffuse in three dimensions away from the release site as Ca^{2+} continues to be discharged. Therefore, to quantify the increase in total fluorescence, i.e., *the Ca^{2+} signal mass* (ΔCaFl) resulting from the binding of fluo-3 to the discharged Ca^{2+}, fluorescence must be collected from a sufficiently large volume surrounding the release site. The optimal value for this volume was determined by the method of ZhuGe et al. (2000) to be that subtended by an area of 116 μm^2 (81 × 81 pixels) (1). Because photons must be collected from a three-dimensional volume and not simply from a single plane, wide-field microscopy that gathers light from the entire thickness of the cell is well suited to this method. To relate measured increase in fluorescence to the total amount of Ca^{2+} released in a single syntilla (Ca_T), a calibration curve was constructed that related measured fluorescence to the amount of Ca^{2+} bound to fluo3 (ΔCaFl) as described previously (1).

Because whole-cell patch recording was employed at the same time that images were acquired, endogenous mobile buffers were dialyzed away through the patch pipette and so can be neglected. In the absence of all other buffers, 50 μM fluo-3 binds >97% of Ca^{2+} entering the cytosol for Ca^{2+} currents ranging from 0.1 to 10 pA (13). Thus the peak signal mass provides a faithful indicator of Ca_T in the absence of buffers other than fluo-3. However, endogenous nonmobile buffers alter the magnitude and time course of the signal mass and hence determinations of Ca_T and Ca^{2+} current underlying a Ca^{2+} syntilla ($I_{Ca(syntilla)}$); these effects can be dealt with at the plateau phase of the signal mass, as described previously (1) by using the binding ratios (κ) of the buffers (15). To obtain the value of κ, we measured the resting [Ca^{2+}] ratiometrically using 50 μM fura-2 in place of fluo-3 in the patch pipette. In Ca^{2+}-free external medium the cytosolic [Ca^{2+}] was 100.1 ± 49.5 nM ($n = 4$), and in the presence of extracellular Ca^{2+}, it was 174.9 ± 91.9 nM ($n = 6$). Based on this we used a value of 100 nM to estimate the values of κ for Fluo-3 and endogenous buffer, which were 38.2 and 42, respectively (16). We also used a value of 100 nM for cytosolic [Ca^{2+}] in our simulations described below.

Simulations of the spatiotemporal profile of [Ca^{2+}] arising from a syntilla

To gain insight into the possible role of syntillas, we modeled a cell and simulated syntillas, and examined the spatial and temporal profile of free [Ca^{2+}] that resulted at the plasma membrane where vesicle fusion would occur. Here we are dealing with a nonequilibrium condition. Finite difference approximations were used to solve a set of partial differential equations for the reaction-diffusion kinetics in a cylindrical coordinate system. The details of this approach are described elsewhere (17), and it has been used before for analyzing the spatial-temporal profile of [Ca^{2+}] resulting from Ca^{2+} sparks in smooth muscle (13,18). The cell was modeled as a cylinder, 6 μm in diameter and 3 μm in height. The Ca^{2+} release site was modeled as a small cylinder, 100 nm in diameter and height, located either directly under the plasma membrane (PM) as shown in the cartoon on the right side of Fig. 3 or at various distances inward from the PM. The simulation included: 1.68 mM of fixed (nondiffusible) buffer ($K_d = 10\ \mu M$, $k_{on} = 5 \times 10^5\ mM^{-1}s^{-1}$, $k_{off} = 5 \times 10^3\ s^{-1}$), 100 μM of a (slowly) diffusible buffer ($K_d = 10\ \mu M$, $k_{on} = 5 \times 10^5\ mM^{-1}s^{-1}$, $k_{off} = 5 \times 10^3\ s^{-1}$, $D = 15\ \mu m^2s^{-1}$), and 4 mM of ATP ($K_d = 2.3$ mM, $k_{on} = 5 \times 10^5\ mM^{-1}s^{-1}$, $k_{off} = 11.5 \times 10^5\ s^{-1}$). The ATP kinetics are adjusted for the presence of Mg^{2+} as in Klingauf and Neher (16). The total concentration of fixed and slowly diffusible buffers and the on and off kinetics were taken to be the same as those determined by Klingauf and Neher (16) in bovine adrenal chromaffin cells.

Immunocytochemistry

Immunocytochemistry was carried out as described previously (1) with preimmune serum used as controls. Polyclonal rabbit antibodies for RyRs were generated using the following epitopes: RREGPRGPHLVGPSRC for RyR1 (19), KAALDFSDAREKKKPKKDSSLSAV for RyR2 (20). The polyclonal rabbit anti-RyR3 antibody was developed against purified

glutathione-*S*-transferase fusion protein corresponding to the region of low homology between the transmembrane domains 4 and 5 of RyR3 (21).

Amperometric detection of catecholamine

Quantal release of catecholamine from single chromaffin cells was monitored electrochemically with carbon fiber electrodes as described before (22,23). The electrode, with a tip diameter of 5.8 μm (ALA Scientific Instruments, Westbury, NY), was positioned in contact with the cell surface to minimize the diffusion distance from release sites. To oxidize released catecholamine, the electrodes were held at +650 mV versus the Ag/AgCl reference electrode in the bath. Amperometric signals, i.e., oxidation currents, were monitored with a VA-10 amplifier (NPI Electronic, Tamm, Germany), filtered at 0.5 kHz, digitized at 1 kHz with a Digidata 1200B acquisition system, and acquired with Clampex software from pClamp 8.1 (Axon Instruments, Sunnyvale, CA). Amperometric spikes were identified and analyzed using the Mini Analysis Program (Synaptosoft, Decatur, GA). Each event was visually inspected so that artifacts, for example, baseline noise from exposure of the carbon fiber to the laser light, could be rejected from the analysis. To minimize errors due to possible variation in exocytosis among cells from different animals, cells from each animal were divided into two groups: one as control and the other treated with agents such as ryanodine.

RT-PCR to detect mRNA for RyRs

The cortex of adrenals was carefully removed and the medullae were then quickly frozen in dry ice. The total RNA of the medullae was isolated with the TRIzol (Invitrogen, Carlsbad, CA) method following the manufacturer's guidelines; and cDNA was synthesized using extracted RNA with an Omniscript Reverse Transcription Kit (Qiagen, Valencia, CA). The specific primers for mouse RyR1, RyR2, RyR3, and for β-actin have been described previously (24) and were synthesized by Invitrogen. β-Actin was used as positive control and the absence of DNA as negative control, and the polymerase chain reaction (PCR) was carried out in a PCR mastercycler (model 5332; Eppendorf, Westbury, NY). The PCR was held at 94°C for 30 s then cycled 35 times, each cycle consisting of: 93°C for 30 s, 54°C for 30 s and 72°C for 30 s.

Data analysis

In all cases data are reported as mean ±SE. Statistical analysis of difference was made with Student's *t*-test and the *p*-values are presented in the figure captions, as appropriate. *N* indicates the number of cells and *n* the number of events, i.e., syntillas or amperometric spikes.

RESULTS

Freshly dissociated chromaffin cells from mice were studied on the same day as isolation; and the results presented in this study derive from a total of 116 chromaffin cells from 35 mice. The cells were patched in whole-cell mode, and the Ca^{2+} indicator, fluo-3, in the salt form (50 μM) was dialyzed from the patch pipette into the cytosol. Unless otherwise indicated, the membrane potential was held at −80 mV, and the extracellular solution was nominally Ca^{2+}-free, with 200 μM EGTA added. Under these conditions we looked for spontaneous Ca^{2+} transients of the type that we have recorded previously in isolated nerve terminals of magnocellular neurons from the mouse hypothalamus. Typical results in chromaffin cells are shown in Fig. 1 *A* where the evolution of a spontaneous Ca^{2+} syntilla is shown using high speed (200 Hz), wide-field microscopy. Because there was no extracellular Ca^{2+} present, the Ca^{2+} syntillas must arise from intracellular stores, as is the case for isolated terminals from hypothalamic neurons in our previous study (1).

The top trace in Fig. 1 *B* indicates the time course of the signal mass, that is, the increase in total fluorescence due to the Ca^{2+} released in a single syntilla; the rate of rise is considerably faster than the rate of decay. As outlined in Materials and Methods, the signal mass at its peak is directly proportional to the total amount of Ca^{2+} released in a syntilla, as opposed to the increase in Ca^{2+} concentration (1,13). Using the appropriate estimates of buffer capacity, the total amount of calcium ions released in this syntilla is calculated to be 234,000. Because the signal mass is an integrated measure giving the increase in the amount of cytosolic Ca^{2+}, the time derivative of this signal mass trace, shown in the bottom panel of Fig. 1 *B*, is a function of the underlying Ca^{2+} flux or Ca^{2+} current ($I_{Ca(syntilla)}$) flowing from the intracellular store into the cytosol, in this case a current that has a peak of 3.7 pA and lasts ~20 ms. In calculating $I_{Ca(syntilla)}$ here, we neglect the fixed buffer so that the trace provides the minimal amplitude and maximal duration of the current. (In Fig. 3 we take into account the kinetics of the buffers to estimate the spatiotemporal profile of the Ca^{2+} concentration.) The distribution of calcium ions released per syntilla in 98 events from 27 cells was well fit by a single exponential (not shown) with a mean ±SE of 288,000 ± 2900 (after correction for fixed buffer). The peak current was 2.9 ± 0.32 pA ($n = 98$; $N = 27$) without correction for fixed buffers (see Discussion). When Ca^{2+} syntillas were examined in the presence of a normal concentration of external Ca^{2+} (2.2 mM), again at a holding potential of −80 mV, neither their frequency (0.23 ± 0.06 vs. 0.35 ± 0.05 s^{-1}, in normal and 0 [Ca^{2+}], respectively) nor signal mass ($34.4 \pm 6.5 \times 10^{-20}$ vs. $44.6 \pm 3.0 \times 10^{-20}$ mol Ca^{2+}, in normal and 0 [Ca^{2+}], respectively) was changed significantly ($p > 0.05$, $N = 14$, $n = 39$ in presence of Ca^{2+}; and $N = 27$, $n = 96$ in the absence of Ca^{2+}). The values for individual syntillas are similar to what we found for syntillas in nerve terminals where the mean number of Ca^{2+} ions per syntilla was ~250,000 and peak $I_{Ca(syntilla)}$, the latter not corrected for fixed buffers, was on average 1.88 pA.

Ca^{2+} syntillas in chromaffin cells are mediated by type 2 and perhaps type 3 ryanodine receptors

To determine whether the syntillas are mediated by ryanodine receptors (RyRs), we first examined the effects of either caffeine or a high concentration of ryanodine that blocks syntillas in nerve terminals (1). The effects are shown in Fig. 1 *C*, where a high concentration of ryanodine blocked the Ca^{2+} syntillas virtually completely in all cells tested. In contrast caffeine had different effects in different cells; in 47% of the cells caffeine increased the frequency of the syntillas without changing their signal mass as shown in

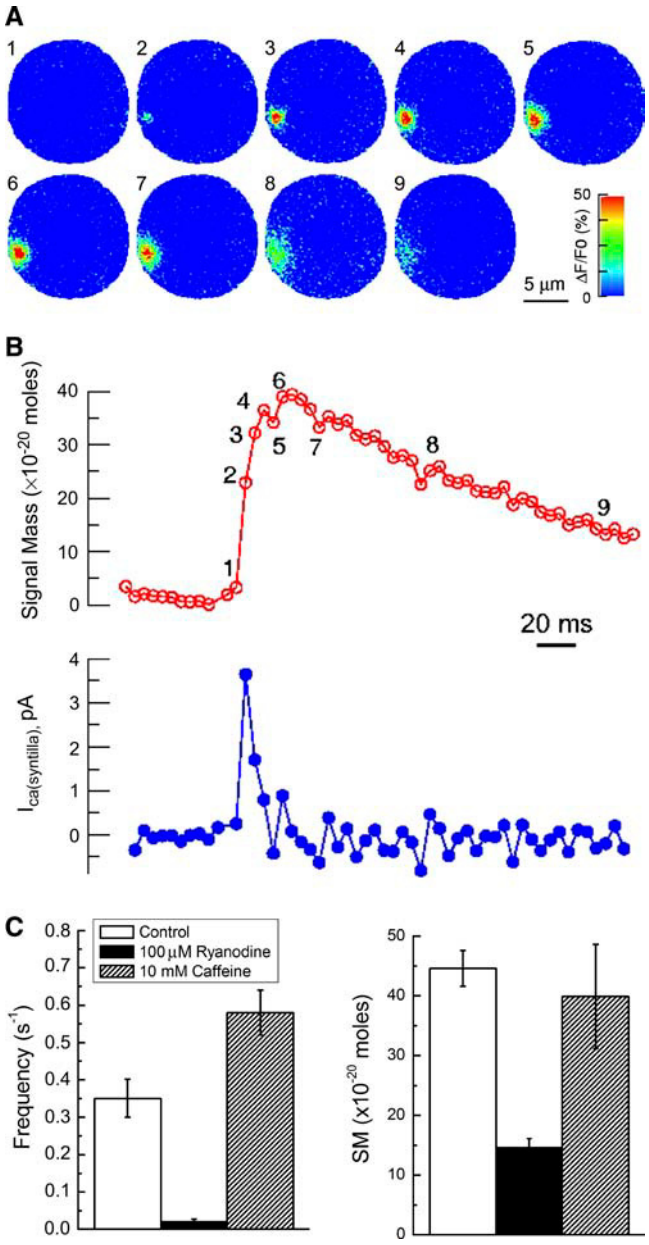

FIGURE 1 Ca^{2+} syntillas result from the opening of RyRs. (*A*) Images display the evolution of a single Ca^{2+} syntilla. Changes in cytosolic Ca^{2+} were measured using fluo-3 (50 μM), which was introduced into the cell in the salt form through the patch pipette. The images were acquired at a rate of 200 Hz with an exposure time of 5 ms. The change in Ca^{2+} concentration in the images is expressed as $\Delta F/F_0$ (%) and displayed on a pseudocolor scale calibrated at the right of the second row of images. Numbers above the images correspond to the numbers in the top part of panel *B* and indicate the time at which the image was obtained. (*B*) The time course of signal mass (*top*) and its time derivative calibrated to give the underlying Ca^{2+} current flowing from the intracellular Ca^{2+} store into the cytosol, i.e., $I_{Ca(syntilla)}$ (*bottom*), for the syntilla shown in panel *A*. (In this calculation of $I_{Ca(syntilla)}$ fixed buffers were not taken into account so that the current trace shown provides the minimum amplitude and maximum duration.) (*C*) The pharmacological properties of Ca^{2+} syntillas. Data shown are Ca^{2+} syntilla frequency (*left*) and amplitude in mol of calcium (*right*) in control conditions or in the presence of 100 μM ryanodine or 10 mM caffeine added to the extracellular solution. The number of cells (*N*) for control, ryanodine, and caffeine treatment is 27, 5, and 11, respectively. For Ca^{2+} syntilla frequency, *p*-values are 0.006 (ryanodine treatment versus control) and 0.008 (caffeine treatment versus control). All Ca^{2+} syntillas were recorded with a high-speed imaging system from chromaffin cells that were voltage-clamped at a holding potential of −80 mV in the absence of extracellular Ca^{2+}.

Fig. 1 *C*. In the remaining 53% of the cells (data not shown) caffeine caused an increase in global $[Ca^{2+}]$, possibly due in part to an even greater increase in syntilla frequency than shown in Fig. 1 *C*. Hence, the effects of caffeine shown in Fig. 1 *C* may be an underestimate. Next we examined the chromaffin cells for the presence of RyRs using both RT-PCR and immunocytochemistry. With RT-PCR (Fig. 2 *A*) we found evidence for both type 2 and type 3 RyRs, but scarcely any indication of type 1. Similarly, immunocytochemistry disclosed clear evidence for type 2 RyRs localized near the plasma membrane, as shown in Fig. 2 *B*, panel *a*, whereas there was no indication of the presence of type 1 (Fig. 2 *B*, *panel b*). Finally, immunocytochemistry disclosed only low levels of type 3 RyRs, and these did not appear to be closely associated with the surface of the cell but rather appeared to lie in the interior of the cell, often in the perinuclear region (Fig. 2 *B*, *panel b*).

In nerve terminals we found that depolarization alone in the absence of Ca^{2+} influx increased syntilla frequency (1). To examine whether the same mechanism is present in chromaffin cells, we applied the experimental paradigm of DeCrescenzo et al. (1) to these cells. We observed that, in the same set of cells, the frequency of syntillas at −80 mV was $1.11 \pm 0.11\ s^{-1}$ ($n = 65$ 3.6-s observation periods in 30 cells) whereas at 0 mV it was $1.11 \pm 0.14\ s^{-1}$ ($n = 60$ 3.6-s observation periods in 30 cells). In contrast, in hypothalamic nerve terminals the syntilla frequency at 0 mV grew so high that it produced global increases (1). The signal mass at −80 and 0 mV in the chromaffin cells was $36.5 \pm 2.1 \times 10^{-20}$ mol ($n = 270$ syntillas in 30 cells) and $28.2 \pm 1.6 \times 10^{-20}$ mol ($n = 280$ syntillas in 30 cells), respectively. Our data indicate that in chromaffin cells, membrane potential by itself did not alter either the syntilla frequency or the number of Ca ions released per syntilla. Corresponding to the failure of depolarization to alter syntilla frequency in chromaffin cells, we find no evidence for type 1 RyRs, the type that mediates direct voltage coupling in skeletal muscle and that we find in abundance in hypothalamic nerve terminals (25).

The spatiotemporal profile of $[Ca^{2+}]$ in the syntilla microdomain

In a number of preparations, it has been suggested that localized presynaptic Ca^{2+} transients cause exocytotic events (8,9). Is this true of Ca^{2+} syntillas in mouse chromaffin cells? Before we approach this question it is desirable to know if the spatiotemporal profile of $[Ca^{2+}]$ resulting from a single syntilla provides enough Ca^{2+} to trigger exocytosis. The signal mass approach allows us to address this question

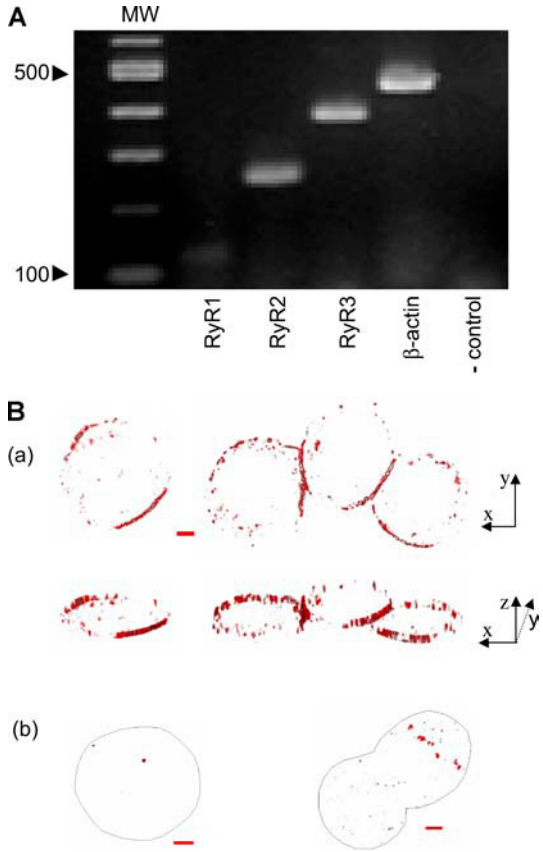

FIGURE 2 Detection and distribution of RyRs. (*A*) RT-PCR detected mRNAs for RyR2 and RyR3 but the signal for RyR1 was scarcely visible. Total RNA was reverse transcribed and the resulting cDNA was amplified by PCR (35 cycles) using primers specific for the mouse RyR mRNA types 1, 2, and 3 (24). (*B*) Immunocytochemistry of isolated chromaffin cells. The images in panel *a* reveal the localization of RyR2 in a section of 1 μm thickness through the middle of the cells (*left*, a single dissociated cell; *right*, a dissociated three-cell cluster). The same images are viewed from two different angles in the top and bottom panels as indicated by the vectors on the right. Note that most of RyR2s are located near the surface. This is especially striking in clusters of cells where the plasma membranes of adjacent cells are closely apposed. In contrast, RyR3s shown in panel *b* (*right*) are located away from the surface, often near the nucleus. Using anti-RyR1 antibodies from two sources, we could not detect RyR1 staining in >40 cells from four animals; an example is shown in panel *b* (*left*) using the anti-RyR1 as previously characterized (19). Black lines in panel *b* were added to indicate the cell outline, which was readily identified in the images before background correction. Bars, 2 μm.

since, together with the measurements of kinetics and capacity of nonmobile buffers in bovine chromaffin cells (16), it permits us to estimate the underlying flow of Ca^{2+} into the cytosol ($I_{Ca(syntilla)}$) and to simulate the spatiotemporal profile of [Ca^{2+}] during a single syntilla (see Materials and Methods). The results are shown in Fig. 3 where the Ca^{2+} current is derived from the signal mass trace, shown in red; the pulse, shown in blue, represents the ''simplest'' form of the underlying current that gives rise to the trace in red as a consequence of filtering by the nonmobile buffers. Aligned temporally with the current in panel *A*, the concentration profiles in panel *B* show the spatial and temporal extent of [Ca^{2+}] when the syntilla arises from a Ca^{2+} store just beneath the plasma membrane. The key point is that the 10-μM isoconcentration line extends 200–300 nm on either side of the release site and persists for ~10 ms. It is estimated that a [Ca^{2+}] on the order of 10 μM is sufficient to cause exocytosis of a docked, primed vesicle in a chromaffin cell (26). A similar profile is given in panel *C*, but here the syntilla site has been moved 300 nm away from the membrane. At this distance there is still a small region of membrane that is exposed to 10 μM [Ca^{2+}]; at greater distances there is no region of membrane exposed to 10 μM (not shown). In summary, if the [Ca^{2+}] release site for a single syntilla lies within 300 nm of a docked, primed vesicle, then exocytosis should occur.

Do single Ca^{2+} syntillas trigger ''spontaneous'' exocytosis of catecholamines in chromaffin cells?

Simultaneous recording of Ca^{2+} syntillas and amperometric events indicates that a single syntilla does not trigger exocytosis. Exocytosis of catecholamines from a single vesicle can be detected amperometrically to determine whether syntillas trigger exocytosis. The rate of syntillas at −80 mV in Ca^{2+}-free external solution is 0.35 ± 0.05 s^{-1} ($N = 27$) and that of recorded amperometric spikes under the same conditions is 0.30 ± 0.12 s^{-1} ($N = 7$) (Fig. 5). But exocytotic events are detected amperometrically only over ~10% of the cell surface nearest the carbon fiber (27), so that the rate of spontaneous exocytosis is on the order of 10 times greater than the rate of syntilla generation; and the occurrence of smaller, nonspike amperometric events would further increase this discrepancy. By this count only one of every 10 syntillas could cause an exocytotic event as measured at the fiber. These data tell us that at most 10% of spontaneous exocytotic events could be caused by syntillas.

We wished to know whether syntillas that occurred in the region of docked and primed vesicles might trigger exocytosis. However, this might represent a small percentage of the apparently spontaneous events and hence would not be apparent from the data in the preceding paragraph. To address this question we examined those syntillas occurring immediately adjacent to the carbon electrode to determine whether they caused exocytotic events or bore any spatiotemporal relationship to them. The placement of the carbon fiber, which was immediately adjacent to the site of the Ca^{2+} syntilla shown, is depicted diagrammatically in Fig. 4 *A*. As can be seen from Fig. 4 *A*, this syntilla did not trigger an amperometric event. A summary of such experiments (Fig. 4 *B*) shows no discernible temporal relationship between syntillas and amperometric events.

The converse experiment is shown in Fig. 4 *C*, where an amperometric spike occurs, but there is no evidence for a syntilla. This experiment addresses the question of whether syntillas cause any appreciable fraction of spontaneous

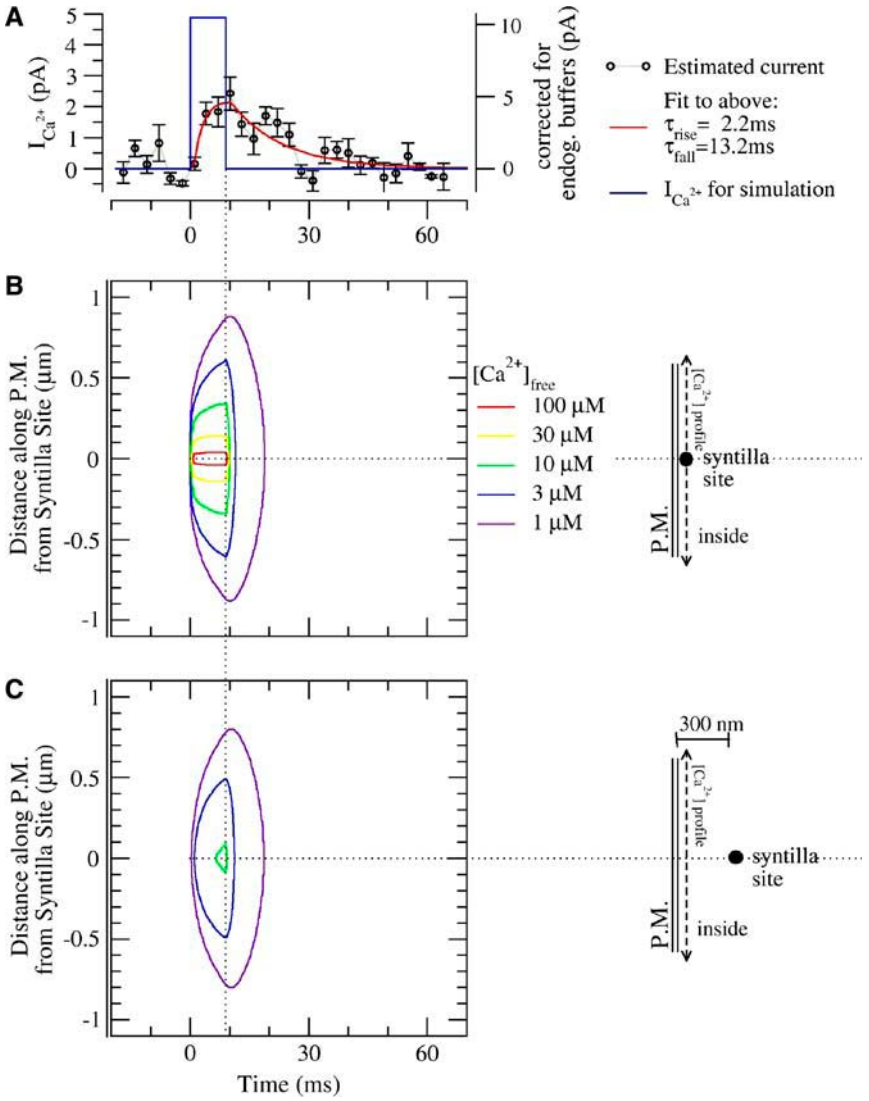

FIGURE 3 Simulations of the spatiotemporal profile of $[Ca^{2+}]$ arising from a syntilla. To gain insight into the possible role of syntillas, we simulated syntillas based on our own signal mass data and published data on buffers in bovine adrenal chromaffin cells (16). (*A*) The I_{Ca} waveform used for simulation (*blue solid line*). The experimentally determined Ca^{2+} current for syntillas recorded at 333 Hz and its best fit are shown in black circles and red solid line, respectively, and referred to the vertical scale on the left. To take into account the additional Ca^{2+} taken up by the endogenous buffers, the amplitude of the Ca^{2+} current was multiplied by the relative buffering capacity of the total endogenous buffer (see Materials and Methods), and this is reflected in the scale on the right and shown as the blue solid line. The selection of square wave as the input to the simulation lies its ''simplest'' waveform, which, when run through the simulation, actually reproduces the fluo3 signal mass time course of the experimental data (the simulated cell acts as a low-pass filter on the input as seen through the fluo3 signal). (*B*) The spatial and temporal profile of free $[Ca^{2+}]$ resulting from a syntilla at the plasma membrane. Isoconcentration lines show the values of free $[Ca^{2+}]$ taken along a line through the center of the release site. The vertical axis is distance along the plasma membrane away from the release site, and the horizontal axis is time. (*C*) The spatiotemporal profile at the plasma membrane due to the same syntilla located 300 nm away from the plasma membrane.

exocytotic events. We observed 124 amperometric events in this sort of experiment ($N = 16$), and we detected a syntilla preceding an amperometric event in only 10 cases. In these 10 cases the latency from syntilla to amperometric event was on average 6.05 s (range 0.97–23.24 s). All 124 amperometric events occurred 0.1 s or later after the onset of the observation period, so that we can say that zero out of 124 events were preceded within 100 ms by a syntilla. These data tell us that $<1\%$ of the syntillas could have triggered an exocytotic event, assuming that the rise in Ca^{2+} must occur within 100 ms before exocytosis (28).

Ryanodine increases the amount of transmitter release in a quantum and abolishes Ca^{2+} syntillas without affecting the rate of spontaneous exocytosis. As shown in Fig. 1 ryanodine (100 μM) almost completely abolished the generation of Ca^{2+} syntillas at -80 mV (0.02 ± 0.01 s^{-1}; $N = 5$). We asked whether the same dose of ryanodine had an effect on spontaneous exocytosis as detected amperometrically. In the presence of ryanodine (100 μM), syntilla frequency was reduced to 6% that of the recorded amperometric events, which as noted above are ~10% of the total (Fig. 5 and Table 1). Thus, only ~0.6% of spontaneous amperometric events can be caused by syntillas. In contrast the frequency of amperometric events was unaffected by this concentration of ryanodine, suggesting that syntillas are not necessary preparatory events for spontaneous exocytosis.

Surprisingly, the amplitude of the spontaneous exocytotic events was increased by 27% in the presence of ryanodine (Table 1). This last finding indicates that the size of the ''quantum'' of transmitter can be substantially altered by a mechanism involving RyRs (see Discussion).

Pharmacological mobilization of Ca^{2+} from stores can elicit exocytosis

Prolonged application of a high concentration of caffeine (10 mM, $N = 8$) can elicit exocytosis as shown in Fig. 6. This is not surprising because a stimulus that raises global $[Ca^{2+}]$

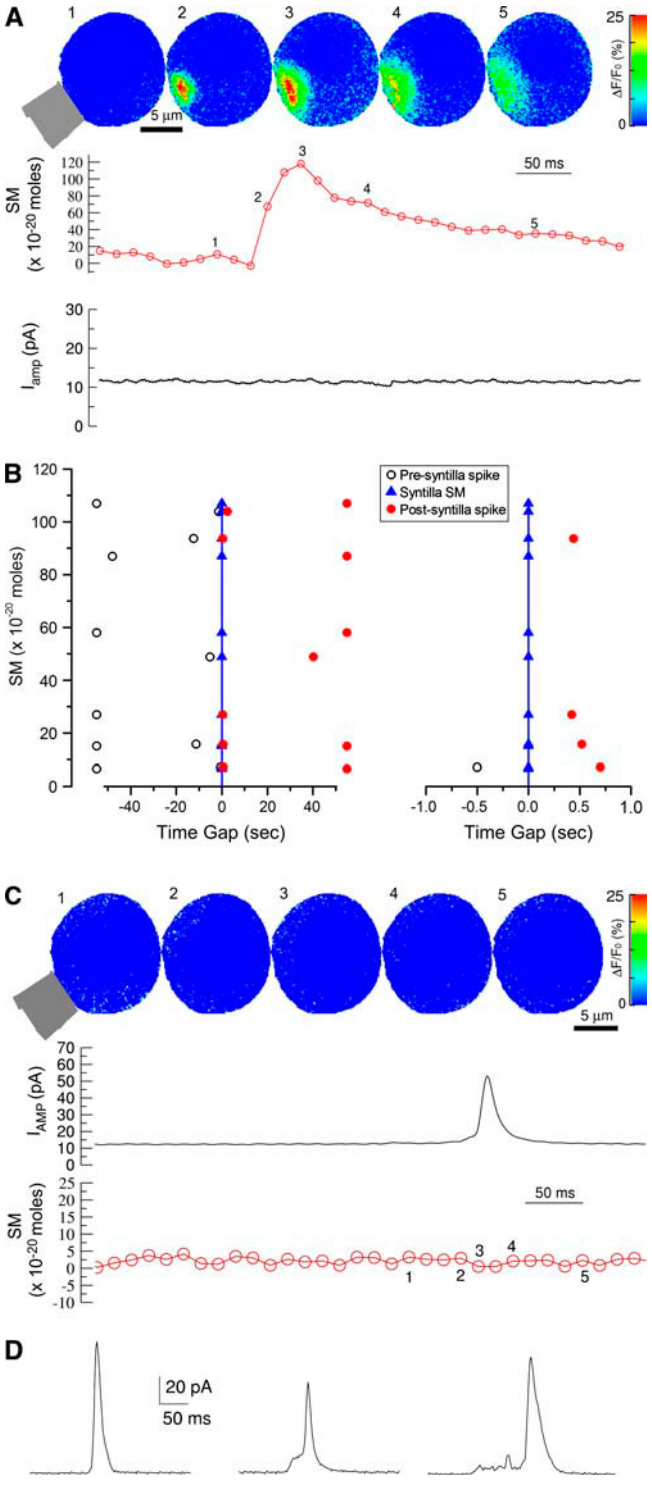

FIGURE 4 Ca^{2+} syntillas do not trigger amperometric events. To simultaneously monitor Ca^{2+} syntillas and exocytotic events, a carbon fiber was placed against the bottom left corner of cells voltage-clamped at the holding potential of −80 mV in the absence of extracellular Ca^{2+} and imaged at a speed of 67 Hz with 5-ms exposure for each image. (*A*) A Ca^{2+} syntilla fails to trigger an exocytotic event. Top panel shows the evolution of a single syntilla adjacent to the carbon fiber (with tip size of 5.8 μm) whose position is depicted at lower left. Traces below show time-integrated trace of total Ca^{2+} released in the syntilla (i.e., the signal mass given in mol of Ca^{2+}) (*middle panel*) and the corresponding amperometric signal recorded at the same time (*bottom panel*). (*B*) Left graph is scatter plot of signal mass for 11 syntillas in eight different cells, and for each syntilla, the closest pre- and postamperometric events in time. Only syntillas occurring immediately adjacent to the carbon fiber (as exemplified in *panel A*) are included in the data. The amplitude of each syntilla is given along the ordinate. Right graph shows short time gap data on an expanded abscissa. (*C*) Amperometric spike (*top trace*) occurring in the absence of a Ca^{2+} transient (*images and bottom trace*). This is the same cell shown in panel *A* with the same conventions as in panel *A*. (*D*) Types of amperometric events that we observed. Note that the ''feet'' of amperometric events with (*right*) and without (*middle*) ''flickers'' were detected.

sufficiently will generate exocytosis whether it is depolarization-induced Ca^{2+} influx, photo release of caged Ca^{2+} or, as here, pharmacological mobilization from intracellular Ca^{2+} stores. Such pharmacological mobilization by itself, however, cannot reveal the physiological function of the syntillas or the stores.

DISCUSSION

Comparison of Ca^{2+} syntillas in nerve terminals and chromaffin cells

The brief, localized Ca^{2+} transients observed in chromaffin cells for the first time in this study are termed Ca^{2+} syntillas, because they resemble those in nerve terminals in a variety of ways. The similarities include: the amount of Ca^{2+} released by an individual syntilla and the exponential distribution of this parameter; the magnitude, rates of rise and decay of the underlying current, $I_{Ca(syntilla)}$; the involvement of RyRs; a basal syntilla rate at −80 mV on the order of 0.5 Hz; and multiple sites of occurrence. In contrast to chromaffin cells, hypothalamic nerve terminals have type 1 RyRs and display regulation of syntilla frequency by membrane potential itself. This suggests that type 1 RyRs may play the same role in neurons that they do in the excitation-contraction mechanism in skeletal muscles; that is, they constitute the target to which dihydropyridine receptors transmit a signal upon depolarization of the plasma membrane, apparently by mechanical coupling between DHPR and RyR1.

Ca^{2+} syntillas arise in a microdomain different from the Ca^{2+} microdomain where Ca^{2+} influx triggers exocytosis

By simultaneously examining individual syntillas and amperometric events, we have found no case where a syntilla triggered exocytosis. The measured rate of amperometric events is ~0.3 s^{-1} for ~10% of the cell surface, or 3 s^{-1} for spontaneous exocytotic events from the whole cell. In the presence of ryanodine (100 μM) the syntilla frequency drops by over an order of magnitude with no change in the rate of amperometric events. Thus, in the presence of 100 μM ryanodine the observed syntilla rate is ~40 times too low to

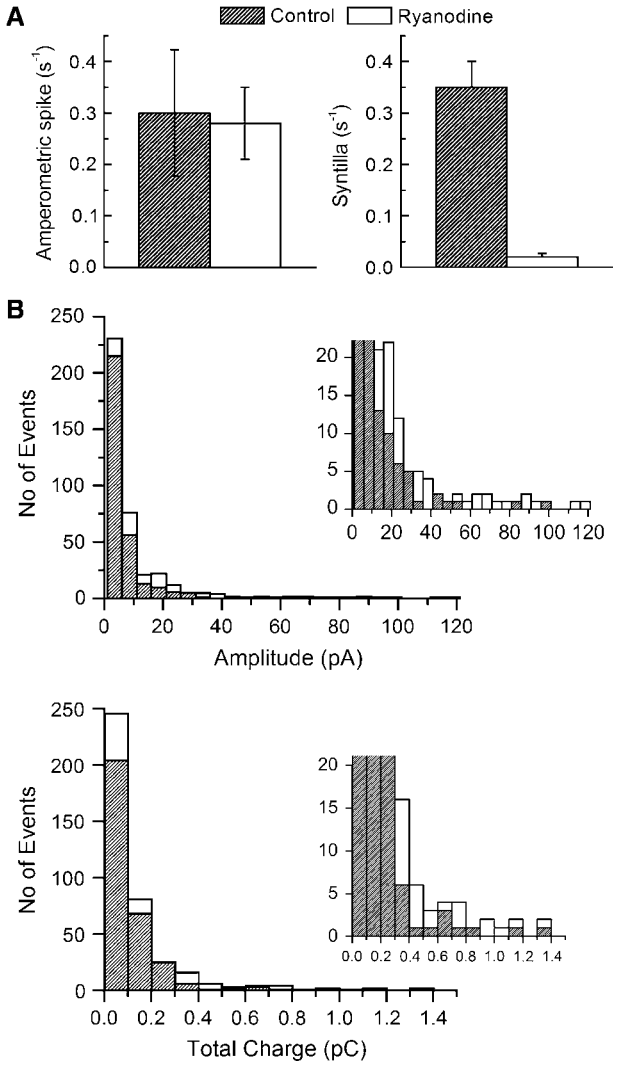

FIGURE 5 Effect of ryanodine on spontaneous exocytotic events and syntilla frequency. Spontaneous spikes were measured from the voltage-clamped cells (holding potential −80 mV) in Ca^{2+} free medium containing 200 μM EGTA and 100 μM ryanodine, after a preincubation for 1 h in normal Ca^{2+} medium with 100 μM ryanodine. Mean values for each parameter and a statistical analysis are given in Table 1. (*A*) Ryanodine does not alter the frequency of spontaneous exocytotic events but reduces the frequency of syntillas >10-fold, virtually abolishing them. (Note that syntilla frequency is for the entire cell whereas the frequency of amperometric events is only for a small region of the cell surface (10%).) (*B*) Ryanodine increases the amplitude of exocytotic events. Top and bottom panels display the amperometric event distributions in terms of amplitude and total charge, respectively. Insets show the same data on an expanded ordinate scale.

account for the observed rate of spontaneous exocytotic events. Recently, using dual wavelength evanescent microscopy and amperometry (29), it has been shown that when a microdomain of $[Ca^{2+}] > 1$ μM arises due to Ca^{2+} influx at the site of a near membrane vesicle in rat chromaffin cells, the probability of exocytosis from that vesicle is 0.1. If all syntillas occurred at the same sites where exocytosis occurs,

TABLE 1 Effect of ryanodine on spontaneous amperometric spikes

	Control	100 μM ryanodine	*p*
Frequency (s^{-1})	0.30 ± 0.1	0.28 ± 0.1	0.92
Amplitude (pA)	7.0 ± 0.6	10.3 ± 0.8	0.0008
Rise time (ms) 10–90	12.9 ± 0.6	12.2 ± 0.5	0.52
Decay (ms)	10.0 ± 0.5	8.8 ± 0.4	0.76
Halfwidth (ms)	23.1 ± 0.9	20.7 ± 0.7	0.92
Total charge (pC)	0.11 ± 0.009	0.14 ± 0.01	0.008

Data were statistically analyzed with Student's *t*-test after log transformation. Control, $N = 7$; $n = 312$. Ryanodine, $N = 5$, $n = 393$.

then the syntilla frequency is 400 times too low to account for the observed rate of amperometric events; that is, only one in 400 exocytotic events can be caused by a syntilla. We conclude that Ca^{2+} syntillas arise at a site distinct from the Ca^{2+} microdomain where the final exocytotic step due to Ca^{2+} influx occurs; there can only be rare exceptions to this fact. The failure of ryanodine to alter the rate of amperometric events despite decreasing the rate of Ca^{2+} syntillas also suggests that syntillas are not involved in any rate-limiting step in mobilizing vesicles for spontaneous exocytosis.

Estimated distance between syntilla microdomain and the microdomain where Ca^{2+} influx and exocytosis occur

Our simulations indicate (Fig. 3) that a syntilla must arise at a site at least 300 nm removed from a docked, primed vesicle. This implies that there is not simply one Ca^{2+} microdomain in excitable exocytotic structures, viz., the microdomain in the vicinity of the plasmalemmal Ca^{2+} channels that trigger the final exocytotic step(s). We suggest that there is at least one other Ca^{2+} microdomain that is not colocalized with docked, primed vesicles. This is similar to the situation that obtains in smooth muscle cells where Ca^{2+} spark sites are localized within 200–300 nm of large-conductance Ca^{2+}-activated K^+ channels (BK channels), exposing them to $[Ca^{2+}]$ on the order of 10 μM. This Ca^{2+} concentration is over an order of magnitude greater than the global $[Ca^{2+}]$ attained in the smooth muscle cell. In this way Ca^{2+} can perform two functions in smooth muscle, with global increases in $[Ca^{2+}] < 1$ μM sufficient to cause contraction but not to activate the BK channels. Conversely, a local increase in $[Ca^{2+}] > 10$ μM at the site of BK channel clusters due to a Ca^{2+} spark can activate BK channels but have no substantial effect on the contractile apparatus (18). The specific target of Ca^{2+} syntillas in nerve terminals or chromaffin cells, the equivalent of BK channels and also Ca^{2+}-activated Cl^- channels (30) is yet to be determined. A hint is provided by the observation that blockade of RyRs with ryanodine results in an increase in the amplitude of the amperometric spikes, suggesting that RyRs are involved in the determination of

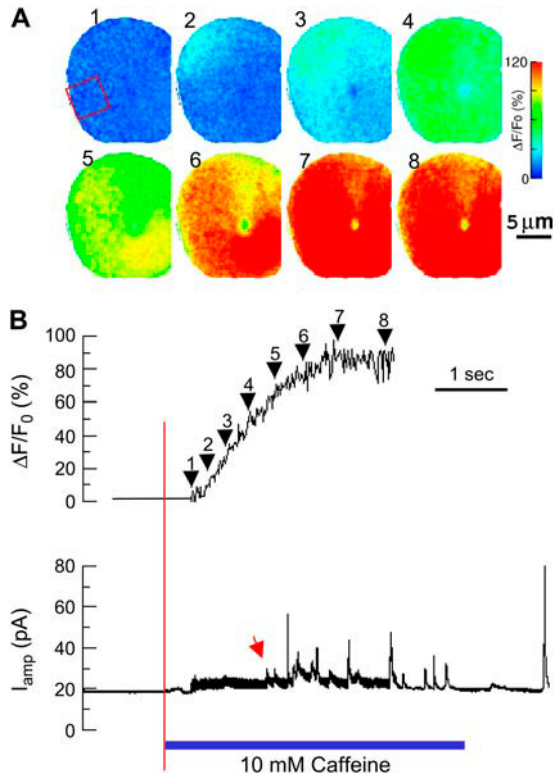

FIGURE 6 Caffeine elicits a rise in global $[Ca^{2+}]$ and exocytosis. (*A*) Images show the development of global increase in $[Ca^{2+}]$ in response to application of caffeine (10 mM) from a nearby pipette. The images were acquired at a rate of 67 Hz with an exposure time of 3 ms per image. The change in Ca^{2+} concentration is expressed as $\Delta F/F_0$ (%) and displayed on a pseudocolor scale calibrated at the right of the images. Numbers above the images correspond to the arrowheads along the line in top panel of *B* and indicate the time at which the image was obtained. The cell was bathed in zero Ca^{2+} medium and held at a membrane potential of −80 mV. Note that a Ca^{2+} syntilla, seen in the upper left corner of the second image in the series, precedes the global increase in $[Ca^{2+}]$. (*B*) The time course of $[Ca^{2+}]$ change in the red box area indicated in panel *A* (*top panel*) and amperometric recording (*bottom panel*) from a carbon fiber positioned against the left side of red box shown in the first image in panel *A*. Vertical red line, indicating onset of caffeine application, aligns the two traces. The blue bar indicates the time of caffeine application. The thickening of the amperometric trace indicates a photoelectric effect at times seen with laser illumination and thus the onset of thickening marks the onset of image acquisition in this series. Note that there was delay of ~1 s before the appearance of the first clear amperometric event (indicated by a *red arrow*) after the onset of the $[Ca^{2+}]$ elevation induced by caffeine.

quantal size, either by regulating the amount of transmitter in a vesicle or by regulating the amount released from the vesicle in a single exocytotic event.

Klingauf and Neher (16) provided a model of the bovine chromaffin cell that explains the relatively long latency of 90% of the exocytosis in response to depolarization-induced Ca^{2+} influx (see also Voets et al. (31)). Here the Ca^{2+} channels are spaced at intervals of several hundred nanometers in the membrane and the docked, primed vesicles are also randomly distributed along the membrane. Only in 10% of the cases do the two coincide, and in these cases exocytosis is of short latency and responsive to a single action potential. In the other 90%, exocytosis occurs after a longer delay and is more responsive to trains of action potentials. (In these cells there is no morphologically identifiable equivalent of an active zone found in neurons (32).) One might ask how syntilla location might fit into such a model. Clearly, as pointed out above, the syntilla sites cannot be targeted to the same site as the docked primed vesicles. Nor does it seem that the syntilla sites can be targeted to the same sites as the Ca^{2+} channels responsible for exocytosis because, in this case, they would cause exocytosis >10% of the time. However, they may well be localized to a different set of Ca^{2+} channels, L-type channels, for example, which would make them sensitive to calcium-induced calcium release from Ca^{2+} influx.

There has long been evidence that the pool of vesicles that underlies spontaneous exocytosis is different from that which accounts for elicited release (33–36). Most recently there is evidence that the molecular machinery for the two types of release is different; and in certain cell types different synaptotagmin isoforms characterize the two pools (37,35, 38). The data in this study suggest that the syntilla sites are not colocalized with the docked, primed vesicles of either pool.

The data here suggest that syntillas do not play a role in mobilizing vesicles for spontaneous release but do not exclude the possibility that they are involved in mobilizing vesicles for elicited release. Hence the syntillas and the Ca^{2+} stores upon which they draw may be responsible for a part of the Ca^{2+}-dependent mobilization of vesicles into the readily releasable pool (39), which in turn has a component dependent on protein kinase C (40) and another independent of it (41,42). The possibility also exists that Ca^{2+} from syntillas can affect the actin network involved in vesicle mobilization (43,44).

Although the concept of multiple Ca^{2+} microdomains can apply readily to a cell the size of a chromaffin cell or even a relatively large neuron terminal, like hypothalamic nerve terminals (1), is it reasonable for smaller central terminals that are 1 μm in diameter and sometimes even smaller? The size of such functional Ca^{2+} microdomains can be shrunk by decreasing the Ca^{2+} affinity of the target molecule. In this connection it is of interest that higher $[Ca^{2+}]$ is required for exocytosis in central neurons such as the ribbon synapse in the retina (45,46). Alternatively, this could be accomplished by altering mobile buffers (47) without any other changes in cellular machinery. But whether further miniaturization is possible and where it is physiologically relevant are questions requiring quantitative information and simulations for Ca^{2+} transients in particular structures. However, it is tempting to envision such microdomains as a way for Ca^{2+} to be employed for several different, perhaps even antagonistic, signaling functions without danger of cross talk.

We thank Jeffrey Carmichael and Yongmei Pei for excellent technical assistance.

This work was supported by grants from National Institutes of Health (HL61297 to J.W. and HL73875 to R.Z.G.) and from The Wellcome Trust to F.A.L.

REFERENCES

1. DeCrescenzo, V., R. ZhuGe, C. Velázquez-Marrero, L. M. Lifshitz, E. Custer, J. Carmichael, F. A. Lai, R. A. Tuft, K. E. Fogarty, J. R. Lemos, and J. V. Walsh Jr. 2004. Ca^{2+} syntillas, miniature Ca^{2+} release events in terminals of hypothalamic neurons, are increased in frequency by depolarization in the absence of Ca^{2+} influx. *J. Neurosci.* 24:1226–1235.
2. Collin, T., A. Marty, and I. Llano. 2005. Presynaptic calcium stores and synaptic transmission. *Curr. Opin. Neurobiol.* 15:275–281.
3. Berridge, M. J. 1998. Neuronal calcium signaling. *Neuron.* 21:13–26.
4. Rose, C. R., and A. Konnerth. 2001. Stores not just for storage: intracellular calcium release and synaptic plasticity. *Neuron.* 31:519–522.
5. Lauri, S. E., Z. A. Bortolotto, R. Nistico, D. Bleakman, P. L. Ornstein, D. Lodge, J. T. Isaac, and G. L. Collingridge. 2003. A role for Ca^{2+} stores in kainate receptor-dependent synaptic facilitation and LTP at mossy fiber synapses in the hippocampus. *Neuron.* 39:327–341.
6. Unni, V. K., S. S. Zakharenko, L. Zablow, A. J. DeCostanzo, and S. A. Siegelbaum. 2004. Calcium release from presynaptic ryanodine-sensitive stores is required for long-term depression at hippocampal CA3–CA3 pyramidal neuron synapses. *J. Neurosci.* 24:9612–9622.
7. Ouardouz, M., M. A. Nikolaeva, E. Coderre, G. W. Zamponi, J. E. McRory, B. D. Trapp, X. Yin, W. Wang, J. Woulfe, and P. K. Stys. 2003. Depolarization-induced Ca^{2+} release in ischemic spinal cord white matter involves L-type Ca^{2+} channel activation of ryanodine receptors. *Neuron.* 40:53–63.
8. Llano, I., J. Gonzalez, C. Caputo, F. A. Lai, L. M. Blayney, Y. P. Tan, and A. Marty. 2000. Presynaptic calcium stores underlie large-amplitude miniature IPSCs and spontaneous calcium transients. *Nat. Neurosci.* 3:1256–1265.
9. Emptage, N. J., C. A. Reid, and A. Fine. 2001. Calcium stores in hippocampal synaptic boutons mediate short-term plasticity, store-operated Ca^{2+} entry, and spontaneous transmitter release. *Neuron.* 29: 197–208.
10. Smith, C. B., and W. J. Betz. 1996. Simultaneous independent measurement of endocytosis and exocytosis. *Nature.* 380:531–534.
11. ZhuGe, R., R. A. Tuft, K. E. Fogarty, K. Bellve, F. S. Fay, and J. V. Walsh Jr. 1999. The influence of sarcoplasmic reticulum Ca^{2+} concentration on Ca^{2+} sparks and spontaneous transient outward currents in single smooth muscle cells. *J. Gen. Physiol.* 113:215–228.
12. Sun, X., P. N. Callamaras, J. S. Marchant, and I. Parker. 1998. A continuum of $InsP_3$-mediated elementary Ca^{2+} signalling events in Xenopus oocytes. *J. Physiol.* 509:67–80.
13. ZhuGe, R., K. E. Fogarty, R. A. Tuft, L. M. Lifshitz, K. Sayar, and J. V. Walsh Jr. 2000. Dynamics of signaling between Ca^{2+} sparks and Ca^{2+}-activated K^+ channels studied with a novel image-based method for direct intracellular measurement of ryanodine receptor Ca^{2+} current. *J. Gen. Physiol.* 116:845–864.
14. Smith, G. D., J. E. Keizer, M. D. Stern, W. J. Lederer, and H. Cheng. 1998. A simple numerical model of calcium spark formation and detection in cardiac myocytes. *Biophys. J.* 75:15–32.
15. Zhou, Z., and E. Neher. 1993. Mobile and immobile calcium buffers in bovine adrenal chromaffin cells. *J. Physiol.* 469:245–273.
16. Klingauf, J., and E. Neher. 1997. Modeling buffered Ca^{2+} diffusion near the membrane: implications for secretion in neuroendocrine cells. *Biophys. J.* 72:674–690.
17. Kargacin, G., and F. S. Fay. 1991. Ca^{2+} movement in smooth muscle cells studied with one- and two-dimensional diffusion models. *Biophys. J.* 60:1088–1100.
18. ZhuGe, R., K. E. Fogarty, R. A.Tuft, and J. V. Walsh Jr. 2002. Spontaneous transient outward currents arise from microdomains where BK channels are exposed to a mean Ca^{2+} concentration on the order of 10 μM during a Ca^{2+} spark. *J. Gen. Physiol.* 120:15–28.
19. Mitchell, K. J., F. A. Lai, and G. A. Rutter. 2003. Ryanodine receptor type I and nicotinic acid adenine dinucleotide phosphate receptors mediate Ca^{2+} release from insulin-containing vesicles in living pancreatic beta-cells (MIN6). *J. Biol. Chem.* 278:11057–11064.
20. Tunwell, R. E., C. Wickenden, B. M. Bertrand, V. I. Shevchenko, M. B. Walsh, P. D. Allen, and F. A. Lai. 1996. The human cardiac muscle ryanodine receptor-calcium release channel: identification, primary structure and topological analysis. *Biochem. J.* 318:477–487.
21. Giannini, G., A. Conti, S. Mammarella, M. Scobogna, and V. Sorrentino. 1995. The ryanodine receptor/calcium channel genes are widely and differentially expressed in murine brain and peripheral tissues. *J. Cell Biol.* 128:893–904.
22. Wightman, R. M., J. A. Jankowski, R. T. Kennedy, K. T. Kawagoe, T. J. Schroeder, D. J. Leszczyszyn, J. A. Near, E. J. Diliberto, Jr., and O. H. Viveros. 1991. Temporally resolved catecholamine spikes correspond to single vesicle release from individual chromaffin cells. *Proc. Natl. Acad. Sci. USA.* 88:10754–10758.
23. Chow, R. H., L. V. Ruden, and E. Neher. 1992. Delay in vesicle fusion revealed by electrochemical monitoring of single secretory events in adrenal chromaffin cells. *Nature.* 356:60–63.
24. Lohn, M., W. Jessner, M. Furstenau, M. Wellner, V. Sorrentino, H. Haller, F. C. Luft, and M. Gollasch. 2001. Regulation of calcium sparks and spontaneous transient outward currents by RyR3 in arterial vascular smooth muscle cells. *Circ. Res.* 89:1051–1057.
25. De Crescenzo, V., R. A. Tuft, K. E. Fogarty, J. D. Carmichael, R. ZhuGe, F. A. Lai, J. R. Lemos, and J. V. Walsh Jr. 2004. Probing How Depolarization Makes Nerve Terminals Syntillate. Program No. 736.14. Abstract Viewer and Itinerary Planner. Society for Neuroscience, San Diego, CA.
26. Voets, T. 2000. Dissection of three Ca^{2+} dependent steps leading to secretion in chromaffin cells from mouse adrenal slices. *Neuron.* 28: 537–545.
27. Haller, M., C. Heinemann, R. H. Chow, R. Heidelberger, and E. Neher. 1998. Comparison of secretory responses as measured by membrane capacitance and by amperometry. *Biophys. J.* 74:2100–2113.
28. Chow, R. H., J. Klingauf, and E. Neher. 1994. Time course of Ca^{2+} concentration triggering exocytosis in neuroendocrine cells. *Proc. Natl. Acad. Sci. USA.* 91:12765–12769.
29. Becherer, U., T. Moser, W. Stuhmer, and M. Oheim. 2003. Calcium regulates exocytosis at the level of single vesicles. *Nat. Neurosci.* 6:846–853.
30. ZhuGe, R., S. M. Sims, R. A. Tuft, K. E. Fogarty, and J. V. Walsh Jr. 1998. Ca^{2+} sparks activate K^+ and Cl^- channels, resulting in spontaneous transient currents in guinea pig tracheal myocytes. *J. Physiol.* 513:711–718.
31. Voets, T., E. Neher, and T. Moser. 1999. Mechanisms underlying phasic and sustained secretion in chromaffin cells from mouse adrenal slices. *Neuron.* 23:607–615.
32. Chow, R. H., J. Klingauf, C. Heinemann, R. S. Zucker, and E. Neher. 1996. Mechanisms determining the time course of secretion in neuroendocrine cells. *Neuron.* 16:369–376.
33. Zengel, J. E., and K. L. Magleby. 1981. Changes in miniature endplate potential frequency during repetitive nerve stimulation in the presence of Ca^{2+}, Ba^{2+}, and Sr^{2+} at the frog neuromuscular junction. *J. Gen. Physiol.* 77:503–529.
34. Goda, Y., and C. F. Stevens. 1994. Two components of transmitter release at a central synapse. *Proc. Natl. Acad. Sci. USA.* 91:12942–12946.
35. Geppert, M., Y. Goda, R. E. Hammer, C. Li, T. W. Rosahl, C. F. Stevens, and T. C. Südhof. 1994. Synaptotagmin I: a major Ca^{2+} sensor for transmitter release at a central synapse. *Cell.* 79:717–727.
36. Sara, Y., T. Virmani, F. Deák, X. Liu, and E. T. Kavalali. 2005. An isolated pool of vesicles recycles at rest and drives spontaneous neurotransmission. *Neuron.* 45:563–573.

37. Voets, T., T. Moser, P. E. Lund, R. H. Chow, M. Geppert, T. C. Sudhof, and E. Neher. 2001. Intracellular calcium dependence of large dense-core vesicle exocytosis in the absence of synaptotagmin I. *Proc. Natl. Acad. Sci. USA*. 98:11680–11685.

38. Fernandez-Chacon, R., A. Königstorfer, S. H. Gerber, J. Garcia, M. F. Matos, C. F. Stevens, N. Brose, J. Rizo, C. Rosenmund, and T. C. Südhof. 2001. Synaptotagmin I functions as a calcium regulator of release probability. *Nature*. 410:41–49.

39. von Ruden, L., and E. Neher. 1993. A Ca-dependent early step in the release of catecholamines from adrenal chromaffin cells. *Science*. 262: 1061–1065.

40. Gillis, K. D., R. Mossner, and E. Neher. 1996. Protein kinase C enhances exocytosis from chromaffin cells by increasing the size of the readily releasable pool of secretory granules. *Neuron*. 16:1209–1220.

41. Smith, C., T. Moser, T. Xu, and E. Neher. 1998. Cytosolic Ca^{2+} acts by two separate pathways to modulate the supply of release-competent vesicles in chromaffin cells. *Neuron*. 20:1243–1253.

42. Smith, C. 1999. A persistent activity-dependent facilitation in chromaffin cells is caused by Ca^{2+} activation of protein kinase C. *J. Neurosci*. 19:589–598.

43. Vitale, M. L., E. P. Seward, and J. M. Trifaró. 1995. Chromaffin cell cortical actin network dynamics control the size of the release-ready vesicle pool and the initial rate of exocytosis. *Neuron*. 14:353–363.

44. Rose, S. D., T. Lejen, L. Zhang, and J. M. Trifaro. 2001. Chromaffin cell F-actin disassembly and potentiation of catecholamine release in response to protein kinase C activation by phorbol esters is mediated through myristoylated alanine-rich C kinase substrate phosphorylation. *J. Biol. Chem*. 276:36757–36763.

45. von Gersdorff, H., and G. Matthews. 1994. Dynamics of synaptic vesicle fusion and membrane retrieval in synaptic terminals. *Nature*. 367:735–739.

46. Augustine, G. J., F. Santamaria, and K. Tanaka. 2003. Local calcium signaling in neurons. *Neuron*. 40:331–346.

47. Neher, E. 1998. Vesicle pools and Ca^{2+} microdomains: new tools for understanding their roles in neurotransmitter release. *Neuron*. 20:389–399.